BBA - Biomembranes 1860 (2018) 544–555

Contents lists available at ScienceDirect

BBA - Biomembranes

journal homepage: www.elsevier.com/locate/bbamem

Direct visualization of the lateral structure of giant vesicles composed of pseudo-binary mixtures of sulfatide, asialo-GM1 and GM1 with POPC

Pablo M. Rodi[a,b], Bruno Maggio[c], Luis A. Bagatolli[a,d,*]

[a] MEMPHYS - Center for Biomembrane Physics, Denmark
[b] Departamento de Física, Facultad de Bioquímica y Ciencias Biológicas, Universidad Nacional del Litoral, Argentina
[c] Departamento de Química Biológica-CIQUIBIC, Facultad de Ciencias Químicas, Universidad Nacional de Córdoba, Argentina
[d] Yachay EP/Yachay Tech University, San Miguel de Urcuqui, Ecuador

ARTICLE INFO

Keywords:
Sphingolipids
Sulfatide
Asialo-GM1
GM1
Giant unilamellar vesicles
LAURDAN GP
Membrane domains
Membrane hydration

ABSTRACT

We compared the lateral structure of giant unilamellar vesicles (GUVs) composed of three pseudo binary mixtures of different glycosphingolipid (GSL), i.e. sulfatide, asialo-GM1 or GM1, with POPC. These sphingolipids possess similar hydrophobic residues but differ in the size and charge of their polar head group. Fluorescence microscopy experiments using LAURDAN and $DiIC_{18}$ show coexistence of micron sized domains in a molar fraction range that depends on the nature of the GSLs. In all cases, experiments with LAURDAN show that the membrane lateral structure resembles the coexistence of solid ordered and liquid disordered phases. Notably, the overall extent of hydration measured by LAURDAN between the solid ordered and liquid disordered membrane regions show marked similarities and are independent of the size of the GSL polar head group. In addition, the maximum amount of GSL incorporated in the POPC bilayer exhibits a strong dependence on the size of the GSL polar head group following the order sulfatide > asialo-GM1 > GM1. This observation is in full harmony with previous experiments and theoretical predictions for mixtures of these GSL with glycerophospholipids. Finally, compared with previous results reported in GUVs composed of mixtures of POPC with the sphingolipids cerebroside and ceramide, we observed distinctive curvature effects at particular molar fraction regimes in the different mixtures. This suggests a pronounced effect of these GSL on the spontaneous curvature of the bilayer. This observation may be relevant in a biological context, particularly in connection with the highly curved structures found in neural cells.

1. Introduction

Glycosphingolipids (GSLs) are ubiquitous components of animal cell membranes [1]. They participate in a wide variety of physiologically relevant phenomena, including cell recognition and signal transduction processes [1,2]. For instance, GSLs containing simple polar head groups are known to stabilize membranes, possibly through inter-lipid hydrogen bonds [3–5]. Neutral and charged GSLs occur in relatively large amounts in specialized membranes in the nervous system such as myelin [6–9]. At present the effects of these lipids on the structure and function of cell membranes remain unclear.

Gangliosides are enriched in nerve cells where they represent between 2% and 10% of total lipids, contributing approximately 30% of the sialic acid content of the neuronal surface [1,5]. Gangliosides contain one or more sialic acid residues attached to a neutral oligosaccharide chain resulting in a series of polar head-groups of different complexity. The hydrophilic portion of these gangliosides reaches a length similar to that of the hydrocarbon portion and, in turn, dramatically influences the surface, thermotropic and topological properties of membranes containing them [1]. In addition, the number and type of carbohydrates in the polar head-group of these GSLs also have a direct influence on the extent of the interfacial hydration or micropolarity of GSL containing membranes [10–14].

Previous work has elucidated relevant biophysical properties of a series of chemically related sphingolipids ranging from sphingosine, ceramide, cerebrosides and sulfatides to complex gangliosides [1,15–17]. In particular, spatially resolved information about the lateral structure of membranes containing some sphingolipids have been reported, both in model systems and natural membranes by performing fluorescence microscopy experiments in giant unilamellar vesicles (GUVs) [18–24]. The most studied sphingolipid using this approach is sphingomyelin, and several papers using GUVs have been reported in the context of liquid immiscibility directly observed in membranes composed of sphingomyelin/DOPC/cholesterol [19,25–27]. In some of

* Corresponding author at: Instituto de Investigación Médica Mercedes y Martin Ferreyra (INIMEC-CONICET-UNC), Friuli 2434, X5016NST Córdoba, Argentina.
E-mail address: lbagatolli@immf.uncor.edu (L.A. Bagatolli).

https://doi.org/10.1016/j.bbamem.2017.10.022
Received 10 August 2017; Received in revised form 23 October 2017; Accepted 24 October 2017
0005-2736/ © 2017 Elsevier B.V. All rights reserved.

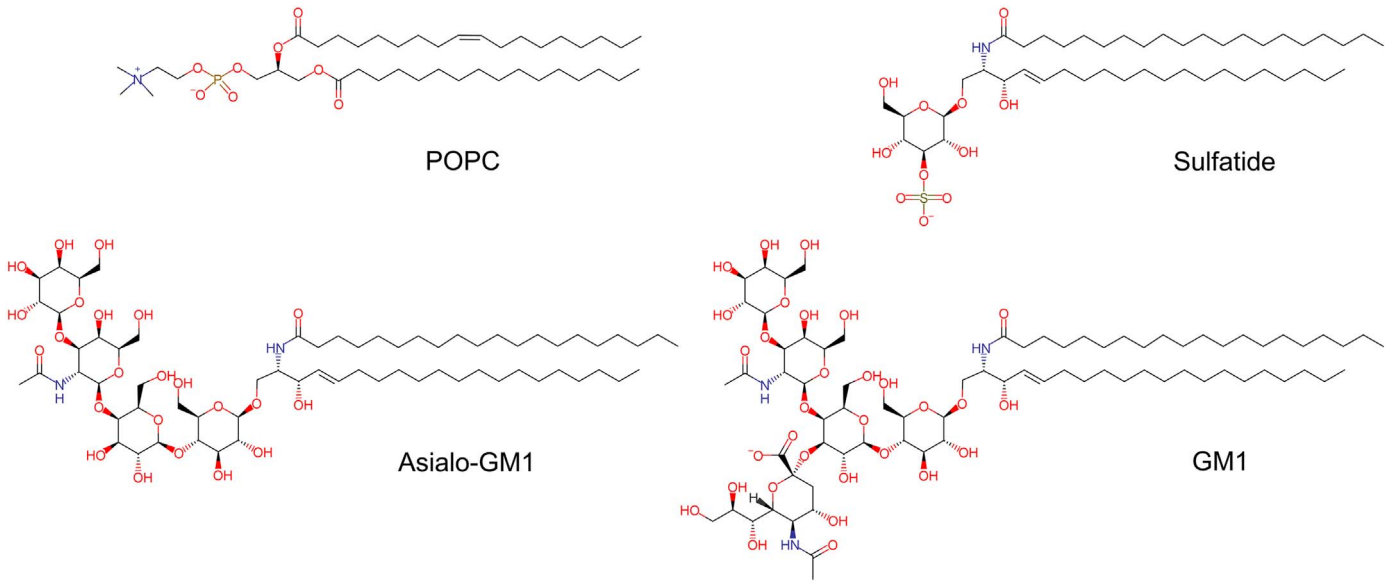

Fig. 1. Molecular structure of Sulfatide, asialo-GM1 (Gg4Cer) and GM1. The molecular structure of POPC is included for comparative purposes (see text).

these studies the ganglioside GM1 has been incorporated in lower proportions to these ternary mixtures mainly as a marker for the liquid ordered phase (using it as a receptor for fluorescently labeled cholera toxin; see for example [27]). However, few studies using microscopy techniques (fluorescence or atomic force microscopy) have addressed about the direct influence of GM1 (or asialo-GM1) on the phase coexistence scenario displayed by this ternary mixture [28–31] or in mixtures with POPC [32].

In this report we study in a comparative manner spatially resolved information obtained by incorporating different proportions of distinct GLS, i.e. GM1, asialo-GM1 (Gg_4Cer) and sulfatide (Fig. 1), in GUVs containing POPC. LAURDAN GP and $DiIC_{18}$ laser scanning confocal fluorescence imaging (one or two photon excitation) are used as the main experimental tool to explore these systems. Our results show a marked effect of these GLSs not only on the lateral structure of the POPC liquid disordered membrane but also on the whole structure of the lamellar system.

2. Materials and methods

2.1. Materials

LAURDAN and $DiIC_{18}$ were purchased from Invitrogen, Denmark. POPC was purchased from Avanti Lipids, Inc. (Alabaster, AL). Lactone-free GM1 from bovine brain was prepared according to Fidelio et al., 1991 [33]. Asialo-GM1 was prepared from the parent GM1 by acid hydrolysis in the presence of DMSO and purified as described by Rodriguez et al., 1996 [34]. Bovine brain sulfatide (3-O-sulfogalactosylceramide) was prepared and purified following the method of Wells & Dittmer 1965 [35]. Substitution of the N-acyl chain by stearic acid was carried out according to Kopaczyc & Radin, 1965 and Carter et al., 1981 [36,37]. HPTLC of each purified lipid in amounts at least 10 times that required for detection showed no contaminant spots after charring the plate with 50% (v/v) H_2SO_4. The composition of the hydrocarbon moiety of each preparation, as determined by GC and HPLC, was as follows: GM1 and asialo-GM1: the sphingoid base was constituted by C18:1-Sphingosine (79.7%), C20:1-Sphingosine (15.6%), C18:1-Sphinganine (4.5%); their N-acyl chain was constituted by C18:0 (95%), C16:0 (2%), C20:0 (1%), C22:0 (1.5%). Sulfatide: the sphingoid base was composed of C18:1-Sphingosine (81.7%), C20:1-Sphingosine (12.6%), C18:1-Sphinganine (2.5%). The N-acyl chain was constituted by C18:0 (90.5%), C24:0 (3%), h-C24:0 (2.5%), C:22:0 (1.6%), C 20:0 (1.8%). To avoid confusions and since each of the glycosphingolipids used in this paper present heterogeneous composition in their hydrophobic moiety, we decided to name their mixtures with POPC as pseudo-binary mixtures.

2.2. Preparation and quantification of lipid stock solutions

GM1 stock solution was prepared in chloroform-methanol-0.01 M NaOH (60:30:4.5) [33] and quantified by the resorcinol/HCl method [38] using Neu5Ac as the reference standards (Sigma Chemical Co.). Similarly, asialo-GM1 stock solution was prepared in chloroform-methanol-0.01 M NaOH (60:30:4.5) and determined by the anthrone-sulfuric acid method [39]. Sulfatide stock solution was prepared in chloroform-methanol-water (2:1:0.1) and quantified according to [40], a colorimetric assay based on the formation of colored salts with methylene blue that are extractable into chloroform. POPC stock in $CHCl_3$ was quantified using phosphorus analysis [41]. Stock solutions for the different pseudo-binary mixtures (0.2 mg/ml) were prepared in chloroform-methanol 2:1 by mixing appropriate aliquots of the different lipid stocks including the fluorescent probes. Probes were 0.1 and 1 mol% with respect to total lipids for DiIC18 and LAURDAN, respectively.

2.2.1. Preparation of GUVs

GUVs were prepared using the electroformation method reported by Angelova et al. [42] using a particular protocol reported elsewhere [20]. Briefly, 3 μl of the lipid mixture's stock solution was spread onto each platinum wire of a special custom built chamber [20] and the organic solvent evaporated using a stream of N_2. After this step, the chamber was placed under vacuum for at least 2 h to remove residual organic solvent. Subsequently, the chamber was assembled and the lipid films hydrated at 70 °C for 15 min using a 0.2 M sucrose solution in presence of an alternate electric field (Amplitude = 2 V and frequency = 10 Hz). The electric field was applied using a function generator (FG100 Vann Draper DigimessFg 100, Stenson, Derby, UK). After this procedure the frequency of the electric field was lowered to 1 Hz for 15 min, in order to detach the vesicles from the Pt wires. Subsequently, the GUVs were cooled to room temperature in a time span of approximately 5 h in an oven (J.P. Selecta, Barcelona, Spain) using a temperature ramp (~0.2 °C/min). This step was done in order to achieve equilibrium conditions in our samples. Once the solution reached room temperature, the vesicles were transferred to an

isoosmolar glucose solution (200 µl of glucose + 50 µl of the GUVs in sucrose) into each of the 8-wells of a plastic chamber (Lab-tek Brand Products, Naperville IL). The density difference between the interior and exterior of the GUVs induces the vesicles to sink to the bottom of the chamber and within a few minutes the vesicles are ready for observation using an inverted microscope. Due to the high temperature used to produce the GUV, which lead to some evaporation of water, the osmolarity of the sucrose solution was measured after GUV preparation. This allows for a careful match with the glucose solution at the temperature of the experiments avoiding undesirable osmotic effects on the GUVs.

2.3. Fluorescence microscopy experiments

An inverted confocal/two photon excitation fluorescence microscope (Zeiss - LSM 510 META NLO, Carl Zeiss, Jena, Germany) was used in our experiments. Two different optical configurations were applied in this system. In the first case we simultaneously excited DiI_{C18} and LAURDAN at 780 nm using two photon excitation fluorescence microscopy by directing the excitation light to the sample using a dichroic mirror (HFTS 690). The excitation source was a Ti:Sa laser Mai Tai XF-W2S (Broadband Mai Tai with 10 W Millennia pump laser, tunable excitation range 710–980 nm, Spectra Physics, Mountain View, CA). For this particular setup the fluorescence emission signals were collected using multitrack mode (included in the Zeiss microscope software) into two different channels using bandpass filters of 590 ± 25 nm and 424 ± 37 nm (for $DiIC_{18}$ and LAURDAN respectively). For the second configuration, which allows only collection of $DiIC_{18}$ fluorescence emission, a laser line of 543 nm was reflected onto the sample using a dichroic mirror (HFST 488/543/633) for excitation and the fluorescence emission was collected using a longpass filter at 560 nm. The objective used in all experiments was a C-Apochromat40X water immersion, NA 1.2. The GUV images included in the figures of this paper are representative of the whole vesicle population (unless indicated) with an average incidence between 70 and 90% depending on the sample. The data were obtained from at least 3 different preparations for each lipid mixture studied (50 to 70 randomly selected GUVs were explored per sample). All the experiments were performed at room temperature (21 °C).

2.4. LAURDAN GP images

The fluorescence emission of LAURDAN is sensitive to the extent of water dipolar relaxation process occurring in the probe's local environment [25,43–46]), which is located at the glycerol backbone region in the phospholipid membrane. The dynamics of water dipolar relaxation occurring in a solid ordered (gel) phase is slow compared with the probe fluorescence lifetime (4×10^{-7} s and 6×10^{-9} s respectively [44,47]) rendering a blue (unrelaxed) fluorescence emission. This phenomenon is different in the liquid disordered phase, where the water relaxation time is in the order of the probe lifetime (2.5×10^{-9} s and 2.6×10^{-9} s respectively [44,47]) rendering a green (relaxed) fluorescence emission. This prominent red shift in the fluorescence emission of the probe, together with the fact that the probe is evenly distributed in membranes showing phase coexistence, allows quantitative detection of different domains with distinct lipid packing [25,43–46]. In order to perform this procedure, the GP function was defined analogously to the fluorescence polarization function as:

$$GP = \frac{I_B - I_R}{I_B + I_R} \quad (1)$$

where I_B and I_R correspond to the intensities at the blue and red edges of the emission spectrum (440 and 490 nm) using a given excitation wavelength [43–46]. Since this function is related to the position of the emission spectra the observed GP values can be directly related with the lateral packing existing in lipid bilayers, allowing spatially resolved information when GP experiments are performed in a microscope. High LAURDAN GP values (0.5–0.6) correspond to laterally ordered phases (solid ordered-like) whereas low LAURDAN GP values (below 0.2) correspond to fluid disordered-like phases [25,43–46].

The LAURDAN Generalized polarization (GP) images of GUVs were obtained using a two photon excitation custom made setup reported elsewhere [48]. Briefly, LAURDAN GP measurements were carried out by means of a custom built multiphoton excitation system constructed in a Nikon Eclipse TI microscope. The objective used was a 60 × water objective with an NA of 1.2. The excitation light source was a femtosecond Ti:Sa laser (HP Mai Tai DeepSee, tunable excitation range 690–1040 nm, Spectra Physics, Mountain View, CA) and the excitation wavelength was 780 nm. The fluorescence signals were collected in two separate detectors by splitting the fluorescence with a dichroic mirror above and below 460 and two bandpass filters of 446 ± 23 nm and 492 ± 23 nm were used (I_B and I_R respectively). To avoid effects of photoselection [25,49] the excitation light was circularly polarized in the x-y plane using a quarter wave plate. The computation of the GP images was performed using MathLab routine. The GP images were calibrated with a correcting G factor as reported elsewhere [50] using a LAURDAN GP standard in DMSO.

3. Results

3.1. Sulfatide/POPC lipid mixtures

Fig. 2 shows representative surface projections of confocal images of GUVs composed of different mixtures of sulfatide with POPC and labeled with fluorescent probe $DiIC_{18}$. The images clearly show three different regimes depending of the sulfatide molar fraction (X_{Sulf}). The first regime occurs when the X_{Sulf} is between 0 and 0.15 and is characterized by a homogeneous distribution of the probe with a very low incidence of domains (Fig. 2a–c) in the vesicle population. The second regime is described by the presence of elongate shaped domains that occur in a very reproducible manner at X_{Sulf} from 0.20 and up to 0.70. In this regime the area fraction of these domains increases steadily by raising the X_{Sulf}. It is worth noting that the partition of the fluorescence probe into these domains does not follow a coherent behavior. At low proportions of sulfatide (X_{Sulf} of 0.05–0.15) the few observed domains arise as brighter areas (Fig. 2a–c) while at X_{Sulf} of about 0.20 these brighter regions are present exclusively at the border of the membrane domains, which display a dark central area (Fig. 2d). When the X_{Sulf} is increased from 0.3 to 0.7 the domains emerge as homogeneous darker areas (Fig. 2e–i). Finally, the third regime occurs above a X_{Sulf} of 0.7 and the domains can be no longer seen (Fig. 2j–l). Similar to the majority of the cases in the first regime, the distribution of the probe at this high X_{Sulf} seems homogenous considering the resolution limit of the optical system (approximately 250 nm radial). In addition, the GUVs appear faceted in this last regime suggesting the presence of crystalline packing in the membrane. In contrast to what was observed in previous studies with GUVs composed of mixtures of POPC with the sphingolipids ceramide and cerebroside [20], we were able to generate GUVs composed of pure sulfatide. It is important to point out, however, that the yield of GUVs at higher proportions of sulfatide (including pure sulfatide) was significantly lower than that observed in the first two regimes, with a high proportion of GUVs displaying a lower average diameter.

In order to further characterize the lateral behavior of this lipid mixture we decided to exploit the fluorescent properties of LAURDAN, which shows important advantages over $DiIC_{18}$. Unlike $DiIC_{18}$, LAURDAN is evenly distributed in membranes displaying lateral heterogeneity and the wavelength of its fluorescence emission depends on the extent of local lipid packing in the membrane (bluish and greenish respectively in the solid ordered and liquid disordered phases [25]; see Material and Methods). First, double labeling experiments with $DiIC_{18}$ and LAURDAN were performed to identify the nature of the different

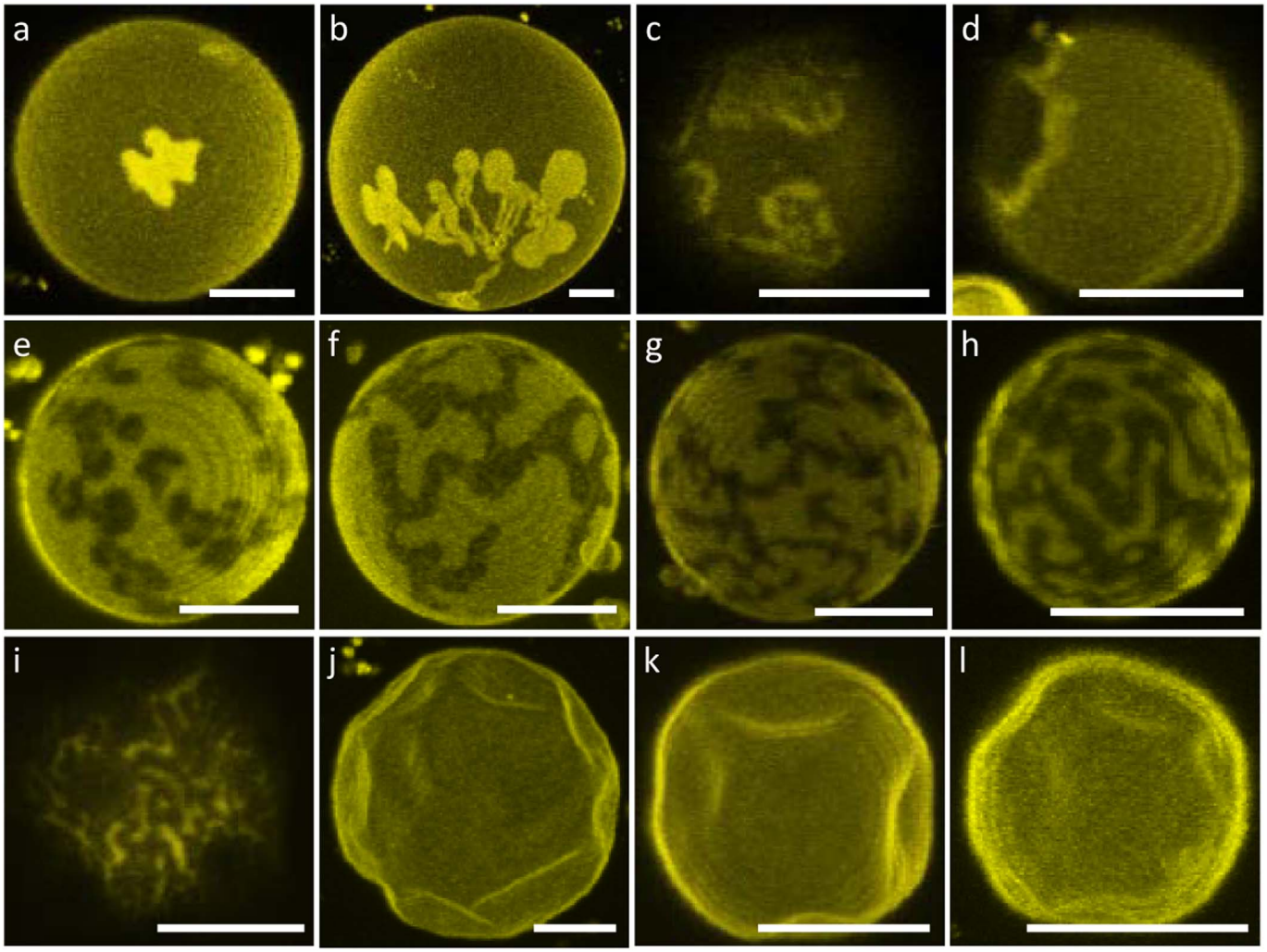

Fig. 2. Representative surface projections of confocal images of sulfatide/POPC GUVs labeled with $DiIC_{18}$. Each image corresponds to mixtures containing different mole fractions of sulfatide (X_{Sulf}): (a) 0.05; (b) 0.10; (c) 0.15; (d) 0.20; (e) 0.30; (f) 0.40; (g) 0.50; (h) 0.60; (i) 0.70; (j) 0.80; (k) 0.90 and (l) 1. Notice that the images included as (a), (b) and (c) are not representative of the whole vesicle population since the presence of domains at this X_{Sulf} was very rare and a frequent incidence of curvature was observed (see text). The experiments were performed at room temperature (21 °C). The white bars correspond to 10 μm.

domains. The trend observed in these experiments was that the domains areas co-localize with a bluish emission of LAURDAN, pointing the presence of crystalline lipid packing in these membrane domains (Fig. S1 for representative examples).

The GP function allows computation of the extent of lipid packing in different membrane regions (see material and methods section, [25,44]). LAURDAN GP images were obtained for GUVs composed of different sulfatide/POPC mixtures and the GP values are presented in Fig. 3 (see also Fig. S2 in the supplementary material illustrating how these values are obtained). From these experiments it can be noticed that the incorporation of low amounts of sulfatide (up to $X_{Sulf} = 0.15$) increases the GP value of the pure POPC membrane with low incidence of micron sized domains. The increase of the GP can be interpreted as an increase in the membrane packing caused by the presence of a lipid with a high melting transition temperature (sulfatide in this case, Tm 50 °C, see [33,51]). Notice that it was not possible to determine with proper statistics the GP values for the domains observed with $DiIC_{18}$ at very low proportion since very few GUVs displayed domains. In addition, although domain coexistence has been detected at $X_{Sulf} = 0.7$ (see Fig. 2i), the LAURDAN GP value for the liquid disordered regions were not included in the figure because the very large error bar in the measured GP for the more liquid areas (notice that only the GP for more ordered areas are included). At this X_{Sulf}, which delimitate the second and third regimes, the liquid disordered areas are very close to the resolution limit of the microscope and it was difficult to obtain statistically meaningful GP values.

On the other hand, the different micron sized membrane regions observed in the GUVs at X_{Sulf} from 0.20–0.60 (Fig. 2c–h) show distinct and steady GP values (domains showing GP values about 0.5 surrounded by areas showing a GP of 0.1 to 0.2 depending of the X_{Sulf}) with a constant ΔGP value (Fig. 3). This observation is in agreement with GP values measured previously in mixtures of POPC and the sphingolipid ceramide that display coexistence of liquid disordered (ld) and solid ordered (so) phases [20]. In light of these observations we can conclude that the solid ordered domains correspond then to sulfatide enriched areas. Notice that the GP values measured for the solid ordered domains at X_{Sulf} from 0.20 to 0.70 remains the same at higher X_{Sulf}. In addition, above $X_{sulf} = 0.7$ the presence of micron sized domains was not detected in agreement with the information provided by $DiIC_{18}$ (Fig. 2j–l) suggesting lipid miscibility between POPC and sulfatide at the resolution limit of our microscopy system (approximately 250 nm radial).

Interestingly, we detected distinct curvature effects in the POPC/sulfatide mixture, which also are dependent on the molar fraction of sulfatide. For example, frequent occurrence of curved structures was observed particularly for relatively low X_{Sulf} (between 0.1 and 0.3),

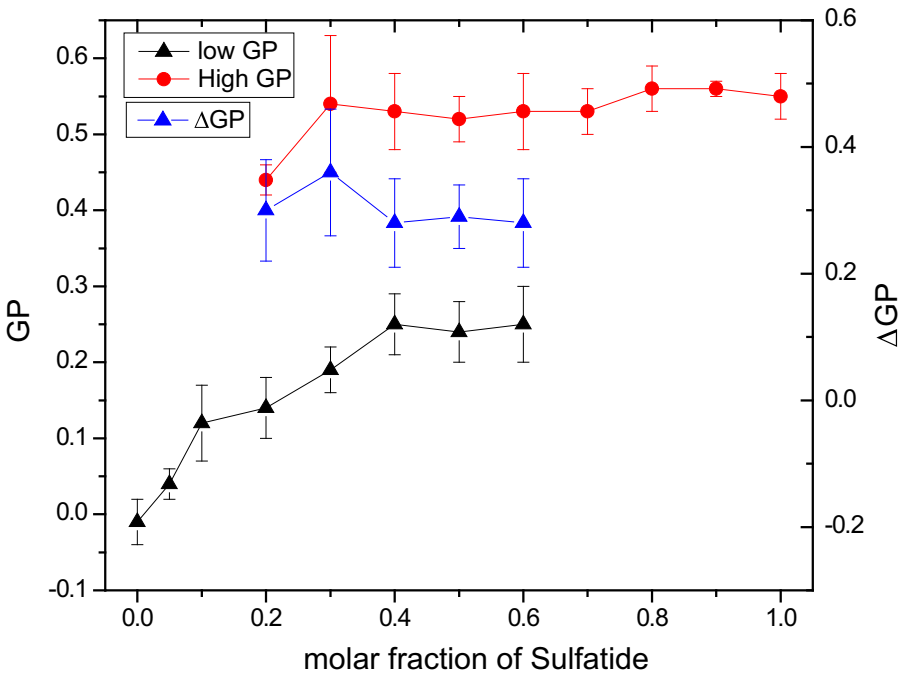

Fig. 3. GP values obtained from LAURDAN GP images of GUVs composed of sulfatide/POPC. The GP values obtained for liquid disordered (black) and solid ordered (red) domains are plotted as a function of sulfatide content. ΔGP (difference between high and low GP values) are also plotted in blue.

Fig. 4a–c. These structures, which deviate from the regular spherical shape generally observed for GUVs, were not detected for GUVs composed of POPC alone (data not shown), suggesting that sulfatides promote these structural disturbances.

Remarkably, this effect disappeared at higher molar fractions of sulfatide, particularly when lipid domains prevail in the bilayer. Instead, the GUVs presents a remarkable local alteration in curvature only at places where sulfatide enriched domains are located (Fig. 4d–f). Finally, at X_{Sulf} above 0.7 this effect is no longer apparent and the GUVs become faceted (Fig. 4 g-I, also evident in Fig. 2j–l), suggesting that crystalline structures dominate the lateral organization of the membrane.

3.2. Asialo-GM1/POPC lipid mixtures

Fig. 5 shows surface projections of confocal sections of asialo-GM1/POPC GUVs labeled with $DiIC_{18}$ showing the presence of elongated micron sized domains. In contrast with the general trend observed for sulfatide/POPC mixtures (Fig. 2) these domains appears always brighter than the surrounded area. In order to identify the lipid packing present in this domains we performed double labeling experiments with $DiIC_{18}$ and LAURDAN. In these experiments the bright fluorescence intensity coming from these domains co-localize with a bluish emission of LAURDAN pointing to the presence of a tight lateral lipid packing (see Fig. S3 supplementary material).

We were unable to detect micron sized lateral heterogeneities below an asialo-GM1 molar fraction (X_{ASG}) of 0.05. At these low asialo-GM1 proportions the GUVs showed an effect of membrane curvature (Fig. S4a) that disappears at higher X_{ASG}. For asialo-GM1 molar fractions from 0.10 to 0.40 the area fraction of these domains increases steadily following the asialo-GM1 proportion in the mixture (Fig. 5a–d). Notice that similar to that observed for sulfatides, the lipid bilayer presents a remarkable alteration in its curvature at places where asialo-GM1 enriched domains are located (Fig. 5b–d, see also Fig. S4b). For higher X_{ASG} (between 0.50 and 0.60) the vesicle surface seems homogenous within the resolution limit of the optical system, showing faceted GUVs (Fig. 5e–f, see also Fig. S4c). At these high asialo-GM1 proportions we observed significant low yield of GUVs with smaller diameters different to that observed at lower proportions of this GSL. Different to that observed for sulfatide it was not possible to observe GUVs above an X_{ASG} of 0.60.

Fig. 6 shows LAURDAN GP values obtained from GP images of GUVs composed of different asialo-GM1/POPC lipid mixtures. The data show that the GP value for pure POPC increases when the X_{ASG} (which has a Tm of 54 °C [33], much higher than POPC) is below 0.1 suggesting the presence of lipid miscibility at the resolution limit of our microscope. At higher X_{ASG} (from 0.1 to below 0.5) the micron sized domains show constant GP values with a ΔGP similar to that observed for the sulfatide/POPC mixture. This suggests the presence of liquid disordered/solid ordered phase coexistence in the membrane with solid ordered domains enriched in asialo-GM1. In addition, the GP values observed for the solid ordered domains show no significant differences considering the experimental error for those measured above X_{ASG} of 0.5 suggesting the existence of miscibility between POPC and asialo-GM1 in a crystalline packing configuration.

3.3. GM1/POPC lipid mixtures

Surface projection of confocal images of GUVs labeled with $DiIC_{18}$ is shown in Fig. 7. It was observed, similar to the case of sulfatide, that these GUVs seldom displayed lateral heterogeneities at low molar fractions (between X_{GM1} of 0 to 0.1 of GM1) (Fig. 7a–b). Above a X_{GM1} of 0.1 on the other hand the appearance of domains was very reproducible in the whole GUV population. These domains showed a preferential partition for $DiIC_{18}$ at any lipid composition in the mixture, with an area fraction increasing steadily as the X_{GM1} increases (Fig. 7a–f). It is worth nothing that these domains show, as in the case of POPC/sulfatide mixtures (Fig. 2c), a fluorescent gradient being slightly brighter at the domains edges (evident in Fig. 7c, dimmer but also present in Fig. 7d–f). Similar to the other two mixtures studied in this paper, GUVs show altered curvature, i.e. relatively low proportion of GM1 (0.05–0.10) yielded curved lamellar structures (Fig. S4d) that gradually disappear when X_{GM1} increases emerging as a local phenomenon at the edge of domains (see Fig. 7b, d–e, see also Fig. S4e). Unlike the others POPC/GSLs mixtures studied in this work, high percentages of GM1 did not promote homogeneous probe distribution, precluding us to elaborate any conclusions about miscibility effects at high X_{GM1}. Also, as in the case of the other POPC/GLS mixtures, a

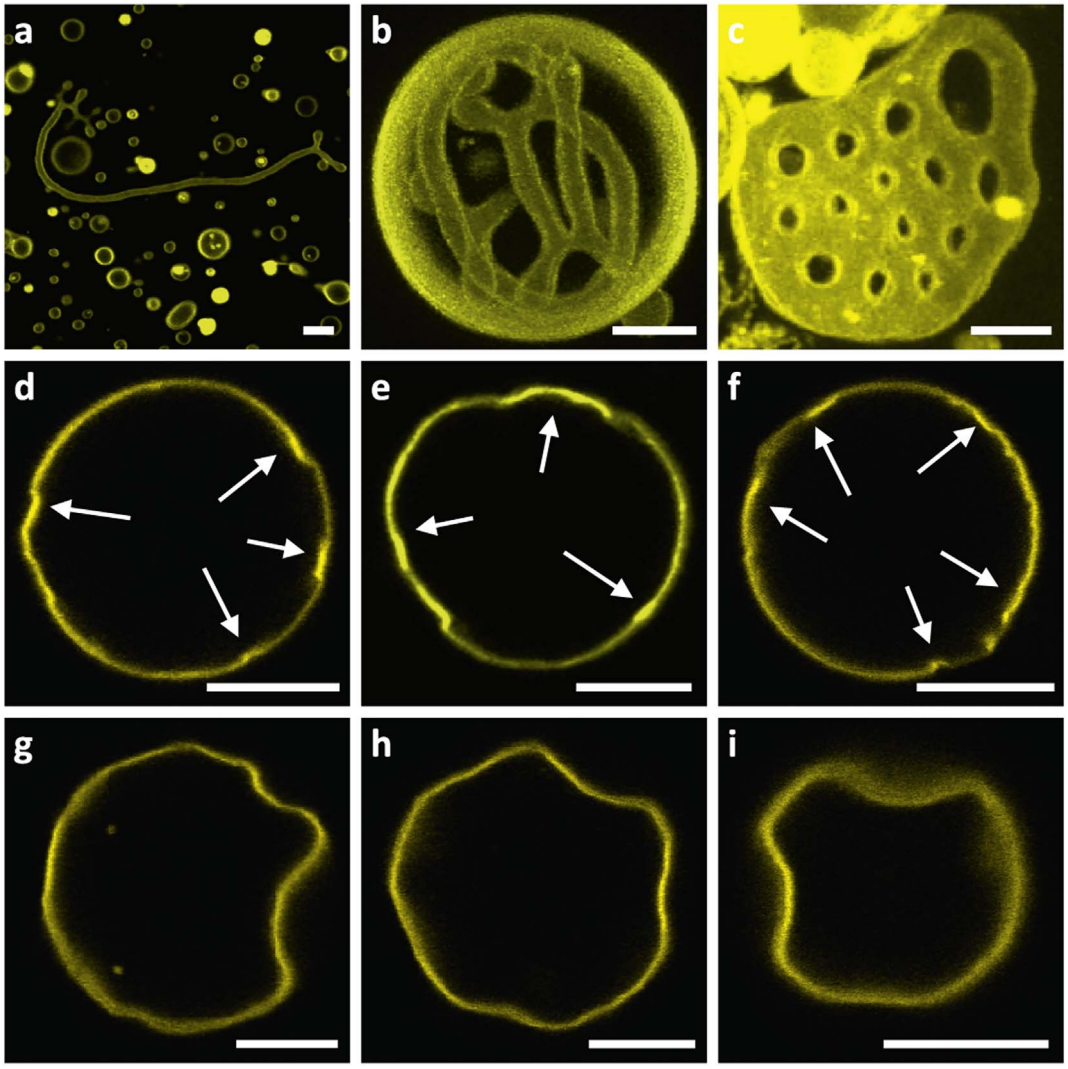

Fig. 4. Distinct effects of curvature promoted by different X_{sulf} in GUVs composed of POPC/sulfatide and labeled with $DiIC_{18}$. (a–c) Surface projections of confocal images showing curvature effects affecting the whole vesicle structure (X_{sulf} below 0.1). (d–f) Confocal images showing curvature effects at the edge of lipid domains (X_{sulf} 0.2–0.6, white arrows). (g–i) Confocal images of faceted vesicles suggesting the presence of crystalline lateral structure (X_{sulf} from 0.7 to 1). Notice that domains are no longer observed at this high proportions of X_{sulf}. Bars correspond to 10 μm.

strong influence of the X_{GM1} on the overall yield of GUVs in the preparation was observed. In this particular case the yield abruptly decreased above a X_{GM1} corresponding to 0.3–0.4. In addition, it was not possible to produce GUVs in mixtures containing a X_{GM1} above 0.50.

By using simultaneous labeling with $DiIC_{18}$ and LAURDAN it was possible to determine that the brighter domains observed with $DiIC_{18}$ co-localize with a bluish emission of LAURDAN. Similar to the case of asialo-GM1, these findings suggest that the brighter domains correspond with crystalline areas enriched in GM1 (see Fig. S3).

Finally, Fig. 8 shows the LAURDAN GP analysis performed as for the other mixtures containing GLS. Again, we can observe that the GP value of pure POPC increases by adding GM1 for X_{GM1} below 0.1 suggesting an impact on the overall lipid packing by the presence of a lipid with a higher transition temperature than POPC (GM1 in this case [33]). Above a X_{GM1} of 0.1 the GP values measured for the coexisting lipid domains remains constant. The steady ΔGP values observed at this molar fraction range, which are very similar to those observed for the other POPC/GSL mixtures, indicate the simultaneous presence of solid ordered and liquid disordered phases in this lipid mixture.

4. Discussion and conclusions

We compared some physical features of GUVs composed of mixtures of sulfatide, asialo-GM1 and GM1 with POPC using fluorescence microscopy. To the best of our knowledge this type of spatially-resolved information does not exist in the literature for pseudo-binary mixtures of these lipids with POPC, except for GM1 [32]. Considering the chemical structure and physicochemical properties of the three GSLs (see Fig. 1) it is possible to obtain interesting insights into the influence of the different chemical moieties [52], i.e. a negatively charged sulfate group (sulfatide), a non-charged and bulky glycosidic group (asialo-GM1) and a negatively charged glycosidic group (GM1), since the hydrophobic part of these molecules is very similar.

4.1. Bilayer stability

We observed a marked difference in ability of these lipids to form bilayer structures when mixed with POPC. For example, while sulfatide formed bilayer structures at all X_{Sulf} (although a decrease in the yield of giant vesicles was observed at very high molar fractions), it was not possible to map the whole GSLs molar range in the mixtures containing

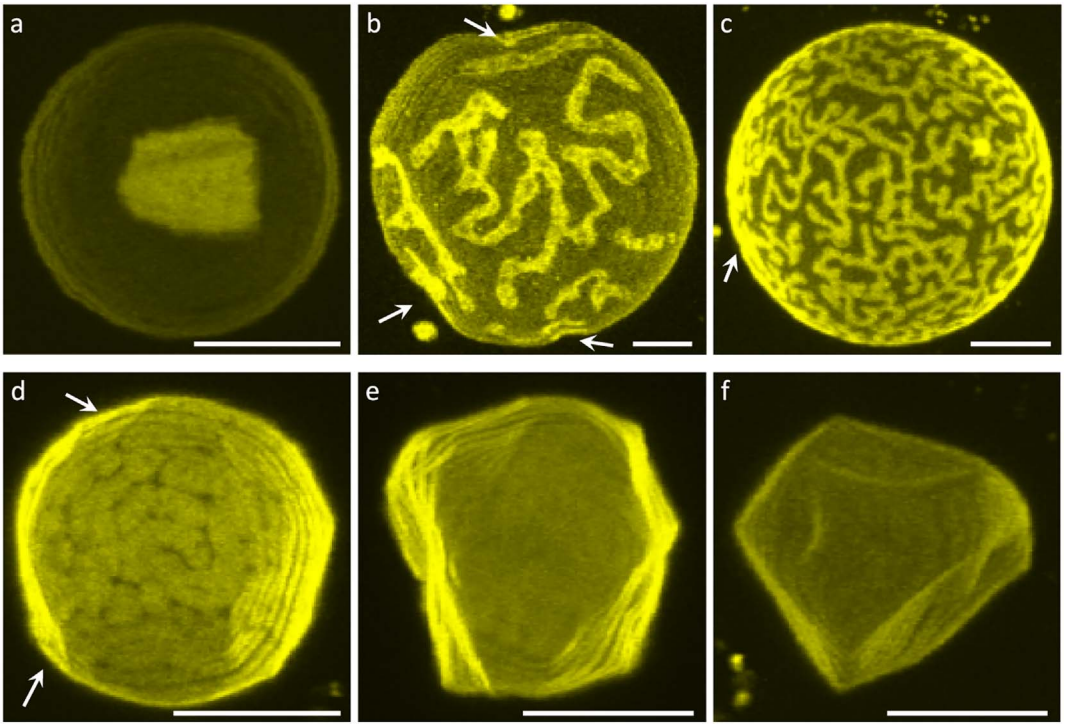

Fig. 5. Representative surface projections of confocal images of asialo-GM1/POPC GUVs labeled with $DiIC_{18}$ at different mole fractions of asialo-GM1 (X_{ASG}): (a) 0.10; (b) 0.20; (c) 0.30; (d) 0.40; (e) 0.50 and (f) 0.60. The white bars correspond to 10 μm. White arrows point altered curvature on domain location.

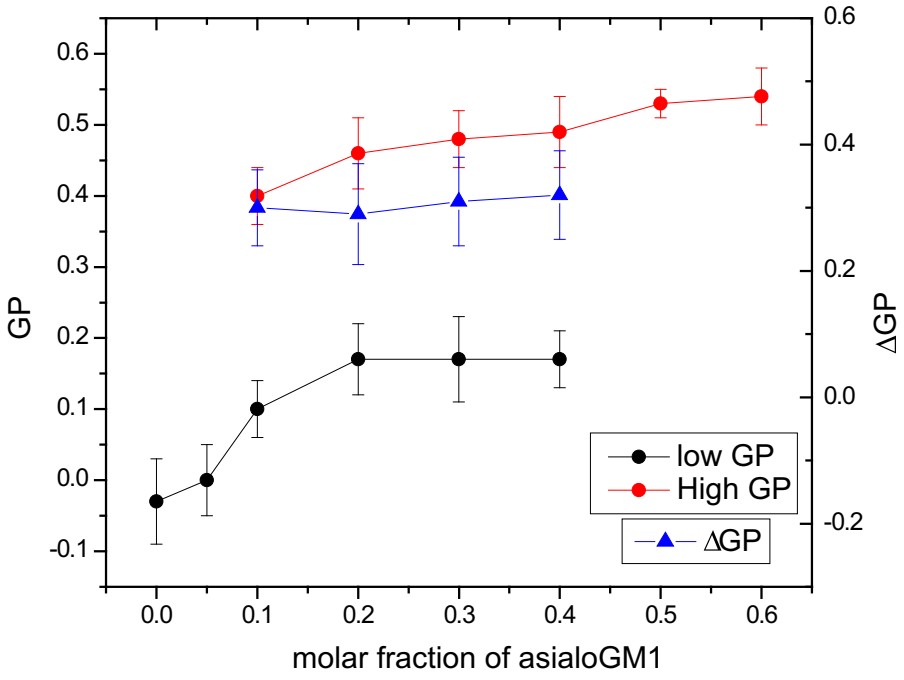

Fig. 6. GP values obtained from LAURDAN GP images of GUVs composed of asialo-GM1/POPC mixtures. The GP values obtained for liquid disordered (black) and solid ordered (red) domains are plotted as a function of asialo-GM1 content. ΔGP (difference between high and low GP values) are also plotted in blue.

asialo-GM1 and GM1, i.e. a marked decrease in the yield of GUVs was observed at higher molar fractions, and above $X_{ASG} = 0.6$ and $X_{GM1} = 0.5$ GUVs were not observed at all. The large curvature imposed by asialo-GM1 and GM1 in bilayers respect to other GSL containing smaller polar head-groups [53] may cause a more prominent positive mean spontaneous curvature [54] promoting the emergence of very curved bilayers and destabilization of the bilayer structure. This gradual decrease in both the overall yield and mean diameter of GUVs could reflect the transition of GUVs from bilayers to nanoscopic non-lamellar structures (micelles), not detectable with optical microscopy, and reported for DPPC/GM1 mixtures using electron microscopy above X_{GM1} of approximately 0.3 [53]. Similarly, it has been reported from electron microscopy experiments that the size of the vesicles composed of asialo-GM1/DPPC mixtures were very small above $X_{ASG} = 0.7$ showing in some cases nanoscopic structures resembling flat stacked disks [53]. Therefore, it seems that the critical packing parameter of

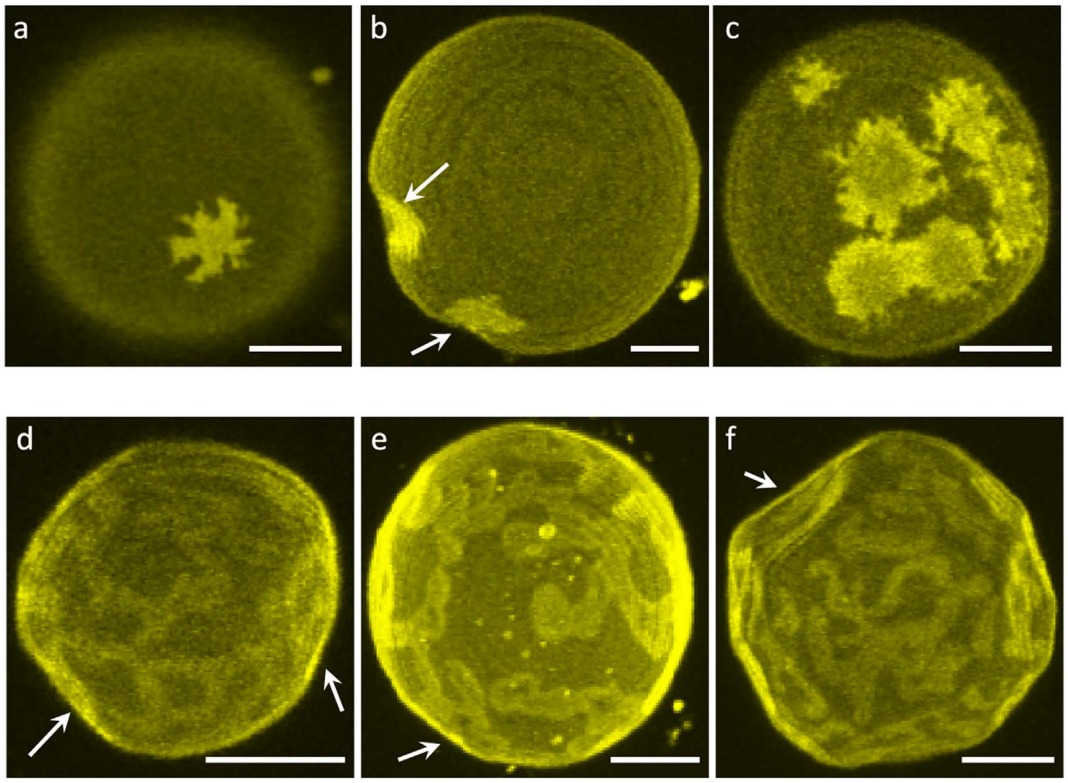

Fig. 7. Representative surface projections of confocal images of GM1/POPC GUVs labeled with $DiIC_{18}$ containing different molar fractions of GM1 (X_{GM1}): (a) 0.05; (b) 0.10; (c) 0.20; (d) 0.30; (e) 0.40 and (f) 0.50. The white bars correspond to 10 μm. Notice that the images included as (a) and (b) are not representative of the whole vesicle population since the presence of domains at this X_{GM1} was very rare. White arrows point altered curvature on domain location.

these lipids is the main reason promoting the pronounced decrease observed in the yield of GUVs at high molar and the impossibility to form GUVs for those holding the bulkier polar head groups. This bilayer stability follows the order sulfatide > asialo-GM1 > GM1 and is in close agreement with previous experiments and theoretical predictions [54]. Finally, it is interesting to note that similar observations have been reported before for other sphingolipids containing GUVs. For example, while the formation of GUVs was observed up to a cerebroside molar fraction of 0.9 in mixtures with POPC (similar to sulfatide) [21], the formation of giant vesicles composed ceramide/POPC mixtures was precluded above 25% mol of ceramide [20], likely related to the well-known tendency of this sphingolipid to form non-lamellar structures.

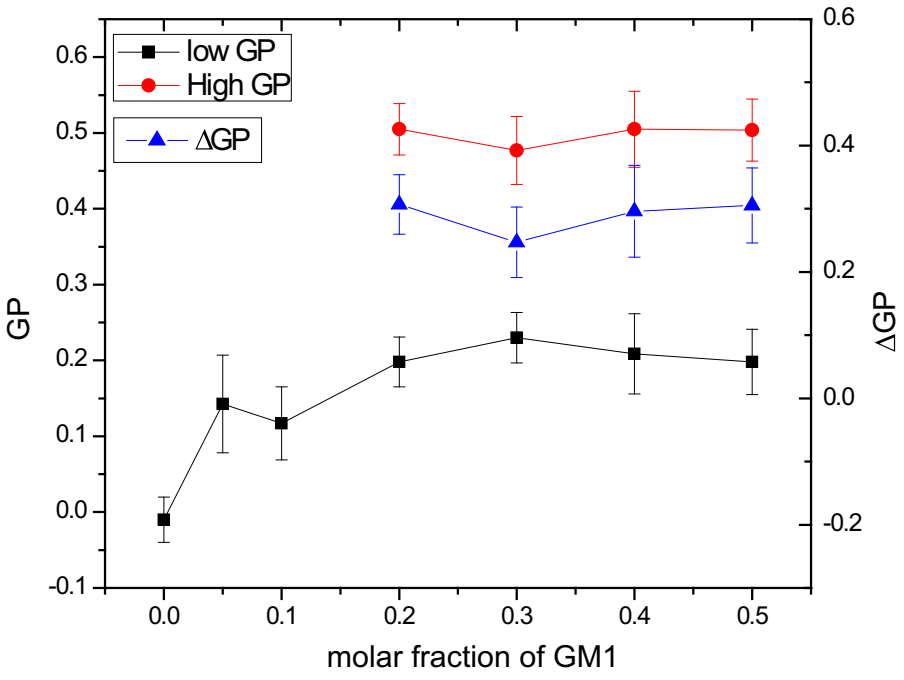

Fig. 8. GP values obtained from LAURDAN GP images of GUVs composed of GM1/POPC mixtures. The GP values obtained for liquid disordered (black) and solid ordered (red) domains are plotted as a function of GM1 content. ΔGP (difference between high and low GP values) are also plotted in blue.

4.2. Spatially resolved information on the lateral structure of GSLs/POPC pseudo binary mixtures

Sulfatide, asialo-GM1 and GM1 have high transition temperatures [51] with respect to POPC, very likely to promote at room temperature lateral heterogeneities in POPC bilayers containing them. Indeed, this was confirmed by our observations. Of particular interest is the spatially resolved information provided here by the fluorescence microscopy experiments. To the best of our knowledge this type of comparative analysis has not been reported before among the mixtures studied in this paper.

We found some similarities but also differences in the lateral structure among these mixtures. The most obvious similitude concerns to the nature of the coexisting phases. Specifically, the three mixtures exhibit coexistence of solid ordered and liquid disordered phases as indicated by LAURDAN experiments (Figs. 3, 6 and 8), in agreement to that reported previously for other lipid mixtures containing sphingolipids [20,21,32]. On the other hand, a noticeable difference was visually spotted by comparing Figs. 2e–i, 5b–d and 7c–f, where phase segregated domains exhibit distinct laterally undulated boundaries for all mixtures which, according to the domain shape transition theory [55], is indicative of marked differences in the resultant dipole moments of the domain phase compared to the surrounding phase [56]. The boundary undulations and/or branching on domains in the mixtures containing the GSL qualitatively agree with previous observations [1,54], increasing in the order sulfatide < Asialo-GM1 < GM1 which is in the same order of the dipole moments of the polar head group of each glycosphingolipid.

The three pseudo binary mixtures also show some similarities concerning the lateral structure exhibited at different molar fractions of the GSLs. For example, lipid miscibility prevails for all mixtures at relatively low molar fractions of GSLs, although the presence of micron sized domains was sporadically observed at this condition for sulfatide and GM1. For these two lipids the upper molar fraction limit observed for this first regime was higher compared with that detected for asialo-GM1 (0.2 vs 0.1 respectively). This peculiar behavior may be related to the presence of a charge effects (sulfatide and GM1) destabilizing the formation of domains at this low molar fractions of GSLs [57]. At this regime all mixtures show a slight increase in LAURDAN GP relative to GUVs composed solely of POPC (Figs. 3 and 6), suggesting an increase in the overall lateral lipid packing in the membrane. This last effect may be linked to energetic considerations concerning the high transition temperature of these lipids relative to POPC [51].

These three mixtures show also similarities at (relative) intermediate molar fractions, a regime that is characterized by the coexistence of solid ordered and liquid disordered phases (Figs. 3, 6, and 8). In this regime the area occupied by the lipid domains gradually increases up to specific molar fractions that depend on the nature of the individual GSL. Notably, the overall extent of hydration measured by LAURDAN for the solid ordered domains shows strong similarities among the mixtures, suggesting a low influence of the GSLs polar head group regulating this parameter (ΔGP, Figs. 3, 6 and 8). Similar ΔGP values using the same experimental approach have been obtained for ceramide/POPC mixtures [20]. This last effect differs to that reported using LAURDAN for lipid aggregates composed of pure asialo-GM1 and GM1 below the main transition temperature, where the LAURDAN GP values show a clear dependence on the nature of the polar head group, i.e. the LAURDAN GP of measured for asialo-GM1 (~0.35) was intermediate between GM1 (~−0.10) and a DPPC bilayer in the solid ordered phase (~0.60) [11]. This discrepancy is due to the nature of the lipid aggregate, i.e. GSL enriched solid ordered domains in a bilayer configuration (data in this paper) vs. ordered structures in a highly curved bilayer or a non-lamellar phase [11].

With exception of GM1, a similar regime occurring at high molar fractions is evident for the mixtures containing asialo-GM1 and sulfatide. In this third regime homogeneous distribution of the probes is observed (Figs. 2j–l and 5e–f), suggesting the presence of lipid miscibility in a membrane displaying a solid ordered phase (Figs. 3 and 6). It is important to emphasize, however, that this observation is limited by the resolution of our microscope (250 nm radial) and in the case of sulfatide partially disagrees with what was observed for DPPC/sulfatide mixtures at high X_{Sulf} [52]. Although POPC differs from DPPC, we cannot rule out the presence of nanoscopic domains in this region. This peculiar transition of the membrane from micron sized domains coexistence to homogeneous distribution of the probes was not detected in similar experiments performed in GUVs composed of binary mixtures of ceramide [20] and cerebroside (GalCer) [21] with POPC.

According to the phase diagram reported by Maggio et al. [52], mixtures of DPPC with the same sulfatide mixture used in this paper show a broad range of temperature and composition where liquid disordered and solid ordered phases coexist. This type of behavior was also reported in mixtures of synthetic sulfatides (24:0) with DPPC [58]. In addition the ability of sulfatide to laterally segregate has been also explored in more complex lipid mixtures [58–61]. For example, bulk suspensions of liposomes composed of POPC/sulfatide/cholesterol (60:30:10 mol) [62] show that sulfatide by itself is able to induce formation of solid ordered phases in the mixture. Similarly, our observation of lateral heterogeneities in GUVs composed of asialo-GM1 and GM1 are in agreement with previous studies that demonstrated i) clustering of asialo-GM1 in small vesicles displaying liquid crystalline bilayers [11,63–65] and ii) phase diagrams obtained by differential scanning calorimetry [52,66] revealing that phase separation of pure DPPC domains showing isothermal melting lead to DPPC-rich or ganglioside-rich mixed domains in the membrane depending on the molar fraction of GM1. In summary, all these results are in line with our experimental observations.

Finally, laterally segregated domains in GUVs composed of mixtures of POPC and GM1 have been recently reported by Fricke et al. [32], where micron sized domains were reported in the mixture up to $X_{GM1} = 0.1$, results which are only in partial agreement with our data. Specifically, we encountered a big difference in the maximum molar fraction of GM1 incorporated in POPC membranes, i.e. $X_{GM1} = 0.1$ from Fricke et al. vs $X_{GM1} = 0.5$ in our experiments. We believe that this difference is related with technical aspects concerning the preparation of the lipid stocks, i.e. not only the solvent used to prepare GM1 stock solutions but the adequate quantification of the lipid concentration in the organic stock solutions. It is well known that a small fraction of aqueous NaOH solution (0.01 M) constitutes a necessary first step to solubilize properly dry GM1 (in powder) before adding the organic mixture chloroform:methanol (final proportion chloroform-methanol-$NaOH_{aq}$ 60:30:4.5 v/v) [33]. The presence of NaOH aqueous solution not only helps to hydrate the bulky hydrophilic polar head group of the lipid (helping to dissolve the lipid in the organic solvent solution), but also protects the lipid to suffer lactonization [33]. This chemical process can drastically change the physicochemical properties of gangliosides affecting as well their interaction with phospholipids [67,68]. Fricke et al. solubilize GM1 directly obtained from the vendor in dichloromethane:methanol after weighting a dry mass of GM1 mixtures, without reporting any further control for quantifying the amount of lipid or its chemical state in the final organic stock solution [32]. In fact, the images shown in their paper at X_{GM1} of 0.1 are very similar to the one we obtained at high proportion of GM1 suggesting an underestimation of the proportion of the ganglioside in the mixture. In addition, previous experiments performed using all-atom molecular-dynamics simulations of GM1 in POPC bilayers up to a X_{GM1} of 0.3 [69] predict the formation of solid ordered domains enriched in GM1, which is in agreement with our observations (Figs. 7 and 8).

4.3. Curvature effects

Remarkably, it was possible to detect pronounced curvature effects in the presence of the three GSLs. For example, our results show

frequent and profound alterations on the whole membrane curvature even at low molar fraction of these lipids, indicating geometrical frustration in the lamellar organization of the membrane (Fig. 4a–c, Fig. S4a and d). This is likely related to spontaneous curvature effects exerted by the presence of these lipids. This effect change at intermediate molar fractions (relative for each GSL), particularly when micron sized lipid domains are prominent in the bilayer. In this particular regime the effect of curvature is confined to local areas near lipid domains (Fig. 4 d-f, Fig. S4b–c and e, also indicated with white arrows in Figs. 5 and 7). Similar effects were observed for POPC/ceramide mixtures in the presence of cholesterol [20], but it was absent in POPC/ceramide or POPC/GalCer mixtures [20,21]. All these results suggest that these GSLs impose strong molecular constraints [54] on the POPC bilayer.

A relevant example of GSLs inducing curvature, which affects the dominant spherical shape of POPC GUVs, is the very peculiar structures observed in the POPC/sulfatide mixtures at low sulfatide molar fractions (particularly Fig. 4b–c). These structures are clear examples of manifestations of the Gaussian curvature modulus (also called saddle-splay modulus), which control the topological complexity of the interface [70]. These effects reflect instabilities on the lamellar structure compensated by local mean curvature such as formation of surfaces of parabolic (i.e. micelles (HI) for pure gangliosides or ganglioside-enriched mixtures) or hyperbolic geometry (i.e. HII for ceramides or sulfatides in certain proportions) that can be induced, facilitated or inhibited by sulfatide and gangliosides depending on their amount in mixtures with phospholipids [71,72]. It should be emphasized that sulfatide, asialo-GM1 and some gangliosides are capable of inducing curvature stress leading to cell-cell and synaptic vesicle-plasma membrane fusion, all phenomena involving non-bilayer membrane intermediates [73–75]. Also, in bilayer phospholipid vesicles, sulfatide and gangliosides can exhibit a dual effect HII-phase formation, membrane fusion and enzyme activities that depend on their proportions by affecting synergistically or antagonistically the membrane curvature [76,77]. All these considerations also rationalize the transition we observed in all mixtures from curved vesicle structures (Fig. 4a–c, Fig. S4 a and d) to local curvature areas near lipid domains in a quasi-spherical GUVs (Fig. 4d–f, Fig. S4b–c and e). Specifically, we propose that this transition could be explained by the phospholipid-driven segregation [52] of large fractions of GSLs molecules into membrane regions displaying a solid ordered phase, an effect that dissipates the curvature stress imposed by the individual GSLs molecules in the whole POPC bilayer.

Although we do not have information on the bilayer leaflet composition for the GUVs used in our experiments, previous work [55] with unilamellar vesicles (40–100 nm in diameter) reported that both sulfatide and GM1 are distributed asymmetrically across the bilayer depending on the proportion of glycosphingolipid in the mixture. The percentage of sulfatide on the outer leaflet varies between 85 and 73% for X_{Sulf} between 0.02 and 04 while for GM1 the figures are between 95 and 80% for X_{GM1} between 0.01 and 0.2; such values closely follow the theoretical predictions based on their critical molecular parameters [59,62]. In these vesicles segregated domains enriched in the glycosphingolipids exist [55]. While a more symmetrical distribution of lipid molecules between the leaflets of the bilayer is expected in the GUVs (because their larger size), compositionally complex samples (as those used here) likely display random local areas inducing compositional asymmetry. In other words, it is unreasonable to expect a 100% compensation when lipids largely deviate from cylindrical symmetry as in the case of our mixtures. The obvious curvature effects we observed are, therefore, likely manifestations of relieving curvature tensions in regions of different lateral (and, concomitantly, transverse) composition.

At high sulfatide and asialo-GM1 content, where lipid miscibility is apparent at the micrometer range (Figs. 2j–l and 4g–i for sulfatide and Fig. 5e–f for asialo GM1) and the membrane is in the solid ordered phase, the GUVs show faceted structures. This type of structure could be related to defects among coexisting neighboring crystalline areas or alternatively crystalline membrane regions coexisting with submicroscopic areas enriched of low melting lipids (POPC). Particularly this last type of morphology has been previously reported in GUVs during DPPC or DMPC phase transitions [78] where the predominant flat crystalline solid ordered phase regions are surrounded by a tiny proportion of flexible liquid disordered regions. However, the observation of faceted GUVs composed solely of sulfatide and the narrow high GP distribution observed in these cases (not shown), supports that this effect may be simply related to defects among coexisting neighboring crystalline areas in the membrane.

4.4. Anomalous partition of the fluorescent marker $DiIC_{18}$

Finally, another interesting feature is the anomalous partition of fluorescent dye $DiIC_{18}$ on sulfatide enriched solid ordered domains, showing high affinity for these domains at relatively low sulfatide proportions, but an important exclusion from these domains when the sulfatide molar fraction increases (Fig. 2). Notice that in contrast, LAURDAN shows unequivocally for all mixtures two coexisting phases when micron size domains are observed, i.e. we did not detect three GP values. It is important to note that, as repeatedly reported, the affinity of particular lipophilic fluorescent dyes (like RhPE, $DiIC_{18}$) is not dependent on the membrane phase but the local lipid composition in the lipid domains [25,44,49,79]. Interestingly, in the case of GUVs composed of POPC/Ceramide or Cerebroside [20,21], the solid ordered sphingolipid enriched domains showed consistently very low partition for $DiIC_{18}$, something that is not observed for the sulfatide. Since $DiIC_{18}$ is negatively charged, the behavior observed in the sulfatide/POPC mixture may indicate charge effects affecting the probe partition. Alternatively, this can be due to the presence of metastability-connected with the composition of the lipid domains- taking place in the mixture. However, the fact that a similar effect (although not so marked as in the case of sulfatide) is apparent in GM1 containing GUVs - which is also charged - but barely present in (neutral) asialo-GM1 containing membranes, favor the presence of charge effects on the anomalous partition of this probe.

Transparency document

The http://dx.doi.org/10.1016/j.bbamem.2017.10.022 associated with this article can be found, in online version.

Acknowledgements

PR thanks FNU, Denmark for support during his postdoctoral fellowship at the University of Southern Denmark. LAB wants to acknowledge the program Prometeo from SENESCYT, Ecuador. BM acknowledges an Emeritus Professorship from the University of Córdoba, Argentina; his research was supported by FONCyT, CONICET and SECyT-UNC, Argentina.

Appendix A. Supplementary data

Supplementary data to this article can be found online at https://doi.org/10.1016/j.bbamem.2017.10.022.

References

[1] B. Maggio, The surface behavior of glycosphingolipids in biomembranes: a new frontier of molecular ecology, Prog. Biophys. Mol. Biol. 62 (1994) 55–117 http://www.ncbi.nlm.nih.gov/pubmed/8085016.
[2] G. Tettamanti, Towards the understanding of the physiological role of gangliosides, New Trends Ganglioside Res. Neurochem. Neuroregenerative Asp. 14 (1988) 625–646.
[3] I. Pascher, Molecular arrangements in sphingolipids conformation and hydrogen bonding of ceramide and their implication on membrane stability and permeability, BBA-Biomembranes 455 (1976) 433–451, http://dx.doi.org/10.1016/0005-2736(76)90316-3.

[4] J.M. Boggs, Lipid intermolecular hydrogen bonding: influence on structural organization and membrane function, Biochim. Biophys. Acta Rev. Biomembr. 906 (1987) 353–404, http://dx.doi.org/10.1016/0304-4157(87)90017-7.

[5] W. Curatolo, The physical properties of glycolipids, Biochim. Biophys. Acta Rev. Biomembr. 906 (1987) 111–136, http://dx.doi.org/10.1016/0304-4157(87)90008-6.

[6] R.W. Ledeen, Biosynthesis, metabolism, and biological effects of gangliosides, Neurobiol. Glycoconjugates, Springer US, Boston, MA, 1989, pp. 43–83, , http://dx.doi.org/10.1007/978-1-4757-5955-6_2.

[7] B. Maggio, G.D. Fidelio, F.A. Cumar, R.K. Yu, Molecular interactions and thermotropic behavior of glycosphingolipids in model membrane systems, Chem. Phys. Lipids 42 (1986) 49–63, http://dx.doi.org/10.1016/0009-3084(86)90042-3.

[8] W.T. Norton, W. Cammer, Isolation and characterization of myelin, Myelin, Springer US, Boston, MA, 1984, pp. 147–195, , http://dx.doi.org/10.1007/978-1-4757-1830-0_5.

[9] R.K. Yu, M. Saito, Structure and localization of gangliosides, Neurobiol. Glycoconjugates, Springer US, Boston, MA, 1989, pp. 1–42, , http://dx.doi.org/10.1007/978-1-4757-5955-6_1.

[10] L.A. Bagatolli, E. Gratton, G.D. Fidelio, Water dynamics in glycosphingolipid aggregates studied by LAURDAN fluorescence, Biophys. J. 75 (1998) 331–341, http://dx.doi.org/10.1016/S0006-3495(98)77517-4.

[11] L.A. Bagatolli, B. Maggio, F. Aguilar, C.P. Sotomayor, G.D. Fidelio, Laurdan properties in glycosphingolipid-phospholipid mixtures: a comparative fluorescence and calorimetric study, Biochim. Biophys. Acta Biomembr. 1325 (1997) 80–90, http://dx.doi.org/10.1016/S0005-2736(96)00246-5.

[12] L.A. Bagatolli, G.G. Montich, M. Ravera, J.D. Perez, G.D. Fidelio, Fatty acid-indole fluorescent derivatives as probes to measure the polarity of interfaces containing gangliosides, Chem. Phys. Lipids 78 (1995) 193–202, http://dx.doi.org/10.1016/0009-3084(95)02499-9.

[13] G.G. Montich, M.M. Bustos, B. Maggio, F.A. Cumar, Micropolarity of interfaces containing anionic and neutral glycosphingolipids as sensed by Merocyanine 540, Chem. Phys. Lipids 38 (1985) 319–326, http://dx.doi.org/10.1016/0009-3084(85)90026-X.

[14] G.G. Montich, J.J. Cosa, B. Maggio, Interaction of 1-anilinonaphthalene 8-sulfonic acid with interfaces containing cerebrosides, sulfatides and gangliosides, Chem. Phys. Lipids 49 (1988) 111–117, http://dx.doi.org/10.1016/0009-3084(88)90072-2.

[15] F.M. Goñi, J. Sot, A. Alonso, Biophysical properties of sphingosine, ceramides and other simple sphingolipids, Biochem. Soc. Trans. 42 (2014) 1401–1408, http://dx.doi.org/10.1042/BST20140159.

[16] B. Westerlund, J.P. Slotte, How the molecular features of glycosphingolipids affect domain formation in fluid membranes, Biochim. Biophys. Acta Biomembr. 1788 (2009) 194–201, http://dx.doi.org/10.1016/j.bbamem.2008.11.010.

[17] S. Sonnino, A. Prinetti, L. Mauri, V. Chigorno, G. Tettamanti, Dynamic and structural properties of sphingolipids as driving forces for the formation of membrane domains, Chem. Rev. 106 (2006) 2111–2125, http://dx.doi.org/10.1021/cr0100446.

[18] Y.J.E. Björkqvist, J. Brewer, L.A. Bagatolli, J.P. Slotte, B. Westerlund, Thermotropic behavior and lateral distribution of very long chain sphingolipids, Biochim. Biophys. Acta Biomembr. 1788 (2009) 1310–1320, http://dx.doi.org/10.1016/j.bbamem.2009.02.019.

[19] C. Dietrich, L.A. Bagatolli, Z.N. Volovyk, N.L. Thompson, M. Levi, K. Jacobson, E. Gratton, Lipid rafts reconstituted in model membranes, Biophys. J. 80 (2001) 1417–1428, http://dx.doi.org/10.1016/S0006-3495(01)76114-0.

[20] M. Fidorra, L. Duelund, C. Leidy, A.C. Simonsen, L.A. Bagatolli, Absence of fluid-ordered/fluid-disordered phase coexistence in ceramide/POPC mixtures containing cholesterol, Biophys. J. 90 (2006) 4437–4451, http://dx.doi.org/10.1529/biophysj.105.077107.

[21] M. Fidorra, T. Heimburg, L.A. Bagatolli, Direct visualization of the lateral structure of porcine brain cerebrosides/POPC mixtures in presence and absence of cholesterol, Biophys. J. 97 (2009) 142–154, http://dx.doi.org/10.1016/j.bpj.2009.03.060.

[22] W.-C. Lin, C.D. Blanchette, M.L. Longo, Fluid-phase chain unsaturation controlling domain microstructure and phase in ternary lipid bilayers containing GalCer and cholesterol, Biophys. J. 92 (2007) 2831–2841, http://dx.doi.org/10.1529/biophysj.106.095422.

[23] S.N. Pinto, L.C. Silva, A.H. Futerman, M. Prieto, Effect of ceramide structure on membrane biophysical properties: the role of acyl chain length and unsaturation, Biochim. Biophys. Acta Biomembr. 1808 (2011) 2753–2760, http://dx.doi.org/10.1016/j.bbamem.2011.07.023.

[24] S.N. Pinto, F. Fernandes, A. Fedorov, A.H. Futerman, L.C. Silva, M. Prieto, A combined fluorescence spectroscopy, confocal and 2-photon microscopy approach to re-evaluate the properties of sphingolipid domains, Biochim. Biophys. Acta Biomembr. 1828 (2013) 2099–2110, http://dx.doi.org/10.1016/j.bbamem.2013.05.011.

[25] L.A. Bagatolli, To see or not to see: lateral organization of biological membranes and fluorescence microscopy, Biochim. Biophys. Acta Biomembr. 1758 (2006) 1541–1556, http://dx.doi.org/10.1016/j.bbamem.2006.05.019.

[26] S.L. Veatch, S.L. Keller, Seeing spots: complex phase behavior in simple membranes, Biochim. Biophys. Acta Mol. Cell Res. 1746 (2005) 172–185, http://dx.doi.org/10.1016/j.bbamcr.2005.06.010.

[27] N. Kahya, D. Scherfeld, K. Bacia, B. Poolman, P. Schwille, Probing lipid mobility of raft-exhibiting model membranes by fluorescence correlation spectroscopy, J. Biol. Chem. 278 (2003) 28109–28115, http://dx.doi.org/10.1074/jbc.M302969200.

[28] N. Puff, C. Watanabe, M. Seigneuret, M.I. Angelova, G. Staneva, Lo/Ld phase coexistence modulation induced by GM1, Biochim. Biophys. Acta Biomembr. 1838 (2014) 2105–2114, http://dx.doi.org/10.1016/j.bbamem.2014.05.002.

[29] G. Staneva, N. Puff, M. Seigneuret, H. Conjeaud, M.I. Angelova, Segregative clustering of Lo and Ld membrane microdomains induced by local pH gradients in GM1-containing giant vesicles: Alipid model for cellular polarization, Langmuir 28 (2012) 16327–16337, http://dx.doi.org/10.1021/la3031107.

[30] R. Bao, L. Li, F. Qiu, Y. Yang, Atomic force microscopy study of ganglioside GM1 concentration effect on lateral phase separation of sphingomyelin/dioleoylphosphatidylcholine/cholesterol bilayers, J. Phys. Chem. B 115 (2011) 5923–5929, http://dx.doi.org/10.1021/jp2008122.

[31] C. Yuan, J. Furlong, P. Burgos, L.J. Johnston, The size of lipid rafts: an atomic force microscopy study of ganglioside GM1 domains in sphingomyelin/DOPC/cholesterol membranes, Biophys. J. 82 (2002) 2526–2535, http://dx.doi.org/10.1016/S0006-3495(02)75596-3.

[32] N. Fricke, R. Dimova, GM1 softens POPC membranes and induces the formation of micron-sized domains, Biophys. J. 111 (2016) 1935–1945, http://dx.doi.org/10.1016/j.bpj.2016.09.028.

[33] G.D. Fidelio, T. Ariga, B. Maggio, Molecular parameters of gangliosides in monolayers: comparative evaluation of suitable purification procedures, J. Biochem. 110 (1991) 12–16 http://www.ncbi.nlm.nih.gov/pubmed/1939017.

[34] P.E. Rodriguez, B. Maggio, F.A. Cumar, Acid and enzymatic hydrolysis of the internal sialic acid residue in native and chemically modified ganglioside GM1, J. Lipid Res. 37 (1996) 382–390 http://www.ncbi.nlm.nih.gov/pubmed/9026535.

[35] M.A. Wells, J.C. Dittmer, A preparative method for the isolation of brain cerebroside, sulfatide and sphingomyelin, J. Chromatogr. A 18 (1965) 503–511, http://dx.doi.org/10.1016/S0021-9673(01)80408-8.

[36] K.C. Kopaczyk, N.S. Radin, In vivo conversions of cerebroside and ceramide in rat brain, J. Lipid Res. 6 (1965) 140–145.

[37] H.E. Carter, J.A. Rothfus, R. Gigg, Biochemistry of the sphingolipids: XII. Conversion of cerebrosides to ceramides and sphingosine; structure of Gaucher cerebroside, J. Lipid Res. 2 (1961) 228–234.

[38] L. Svennerholm, Quantitive estimation of sialic acids, Biochim. Biophys. Acta 24 (1957) 604–611, http://dx.doi.org/10.1016/0006-3002(57)90254-8.

[39] T.a. Scott, E.H. Melvin, Determination of dextran with anthrone, Anal. Chem. 25 (1953) 1656–1661, http://dx.doi.org/10.1021/ac60083a023.

[40] T.H. Haines, A microbial sulfolipid. I. Isolation and physiological studies, J. Protozool. 12 (1965) 655–659, http://dx.doi.org/10.1111/j.1550-7408.1965.tb03268.x.

[41] G.R. Bartlett, Phosphorus assay in column chromatography, J. Biol. Chem. 234 (1959) 466–468.

[42] M.I. Angelova, S. Soleau, P. Méléard, Preparation of giant vesicles by external AC electric fields. Kinetics and applications, Trends Colloid. 89 (1992) 127–131, http://dx.doi.org/10.1007/BFb0116295.

[43] T. Parasassi, E.K. Krasnowska, Laurdan and Prodan as polarity-sensitive fluorescent membrane probes, J. Fluoresc. 8 (1998) 365–373, http://dx.doi.org/10.1023/A:1020528716621.

[44] L.A. Bagatolli, LAURDAN fluorescence properties in membranes: a journey from the fluorometer to the microscope, in: Y. Mély, G. Duportail (Eds.), Fluoresc. Methods to Study Biol. Membr, Springer Berlin Heidelberg, 2013, pp. 3–35 https://link.springer.com/chapter/10.1007%2F4243_2012_42.

[45] T. Parasassi, G. De Stasio, G. Ravagnan, R.M. Rusch, E. Gratton, Quantitation of lipid phases in phospholipid vesicles by the generalized polarization of Laurdan fluorescence, Biophys. J. 60 (1991) 179–189, http://dx.doi.org/10.1016/S0006-3495(91)82041-0.

[46] T. Parasassi, G. De Stasio, A. d'Ubaldo, E. Gratton, Phase fluctuation in phospholipid membranes revealed by Laurdan fluorescence, Biophys. J. 57 (1990) 1179–1186, http://dx.doi.org/10.1016/S0006-3495(90)82637-0.

[47] T. Parasassi, E. Gratton, Packing of phospholipid vesicles studied by oxygen quenching of Laurdan fluorescence, 2 (1992).

[48] T. Bhatia, F. Cornelius, J. Brewer, L.A. Bagatolli, A.C. Simonsen, J.H. Ipsen, O.G. Mouritsen, Spatial distribution and activity of Na(+)/K(+)-ATPase in lipid bilayer membranes with phase boundaries, Biochim. Biophys. Acta 1858 (2016) 1390–1399, http://dx.doi.org/10.1016/j.bbamem.2016.03.015.

[49] L.A. Bagatolli, E. Gratton, Direct observation of lipid domains in free-standing bilayers using two-photon excitation fluorescence microscopy, J. Fluoresc. 11 (2001) 141–160, http://dx.doi.org/10.1023/A:1012228631693.

[50] J. Brewer, J. Bernardino de la Serna, K. Wagner, L.A. Bagatolli, Multiphoton excitation fluorescence microscopy in planar membrane systems, Biochim. Biophys. Acta 1798 (2010) 1301–1308, http://dx.doi.org/10.1016/j.bbamem.2010.02.024.

[51] B. Maggio, T. Ariga, J.M. Sturtevant, R.K. Yu, Thermotropic behavior of glycosphingolipids in aqueous dispersions, Biochemistry 24 (1985) 1084–1092 http://www.ncbi.nlm.nih.gov/pubmed/4096890.

[52] B. Maggio, T. Ariga, J.M. Sturtevant, R.K. Yu, Thermotropic behavior of binary mixtures of dipalmitoylphosphatidylcholine and glycosphingolipids in aqueous dispersions, Biochim. Biophys. Acta 818 (1985) 1–12, http://dx.doi.org/10.1016/0005-2736(85)90131-2.

[53] B. Maggio, J. Albert, R.K. Yu, Thermodynamic-geometric correlations for the morphology of self-assembled structures of glycosphingolipids and their mixtures with dipalmitoylphosphatidylcholine, Biochim. Biophys. Acta 945 (1988) 145–160, http://dx.doi.org/10.1016/0005-2736(88)90477-4.

[54] B. Maggio, M.L. Fanani, C.M. Rosetti, N. Wilke, Biophysics of sphingolipids II. Glycosphingolipids: an assortment of multiple structural information transducers at the membrane surface, Biochim. Biophys. Acta Biomembr. 1758 (2006) 1922–1944, http://dx.doi.org/10.1016/j.bbamem.2006.04.020.

[55] H.M. McConnell, Harmonic shape transitions in lipid monolayer domains, J. Phys. Chem. 94 (1990) 4728–4731, http://dx.doi.org/10.1021/j100374a065.

[56] M.L. Fanani, L. De Tullio, S. Hartel, J. Jara, B. Maggio, Sphingomyelinase-induced

domain shape relaxation driven by out-of-equilibrium changes of composition, Biophys. J. 96 (2009) 67–76, http://dx.doi.org/10.1529/biophysj.108.141499.
[57] G. Gupta, A. Surolia, Glycosphingolipids in microdomain formation and their spatial organization, FEBS Lett. 584 (2010) 1634–1641, http://dx.doi.org/10.1016/j.febslet.2009.11.070.
[58] J.M. Boggs, D. Mulholland, K.M. Koshy, Mixtures of semisynthetic species of cerebroside sulfate with dipalmitoyl phosphatidylcholine. Thermotropic phase behavior and permeability, Biochem. Cell Biol. 68 (1990) 70–82 http://www.ncbi.nlm.nih.gov/pubmed/2350503.
[59] P. Viani, S. Marchesini, G. Cervato, B. Cestaro, Calorimetric properties of mixtures of distearoylphosphatidylcholine and sulfatides with definite fatty acid composition, Biochem. Int. 12 (1986) 125–135 http://www.ncbi.nlm.nih.gov/pubmed/3947371.
[60] J.M. Boggs, K.M. Koshy, G. Rangaraj, Thermotropic phase behavior of mixtures of long chain fatty acid species of phospholipid, Biochemistry 32 (1993) 8908–8922.
[61] W. Weerachatyanukul, I. Probodh, K. Kongmanas, N. Tanphaichitr, L.J. Johnston, Visualizing the localization of sulfoglycolipids in lipid raft domains in model membranes and sperm membrane extracts, Biochim. Biophys. Acta Biomembr. 1768 (2007) 299–310, http://dx.doi.org/10.1016/j.bbamem.2006.08.022.
[62] Y.J.E. Björkqvist, S. Nybond, T.K.M. Nyholm, J.P. Slotte, B. Ramstedt, N-palmitoylsulfatide participates in lateral domain formation in complex lipid bilayers, Biochim. Biophys. Acta Biomembr. 1778 (2008) 954–962, http://dx.doi.org/10.1016/j.bbamem.2007.12.016.
[63] T.W. Tillack, M. Wong, M. Allietta, T.E. Thompson, Organization of the glycosphingolipid asialo-GM1 in phosphatidylcholine bilayers, BBA-Biomembranes. 691 (1982) 261–273, http://dx.doi.org/10.1016/0005-2736(82)90415-1.
[64] P. Rock, M. Allietta, W.W. Young, T.E. Thompson, T.W. Tillack, Ganglioside GM1 and asialo-GM1 at low concentration are preferentially incorporated into the gel phase in two-component, two-phase phosphatidylcholine bilayers, Biochemistry 30 (1991) 19–25, http://dx.doi.org/10.1021/bi00215a003.
[65] R.E. Brown, T.E. Thompson, Spontaneous transfer of ganglioside GM1 between phospholipid vesicles, Biochemistry 26 (1987) 5454–5460, http://dx.doi.org/10.1021/bi00391a036.
[66] L.O. Sillerud, D.E. Schafer, R.K. Yu, W.H. Konigsberg, Calorimetric properties of mixtures of ganglioside GM1 and dipalmitoylphosphatidylcholine, J. Biol. Chem. 254 (1979) 10876–10880 http://www.ncbi.nlm.nih.gov/pubmed/583047 (accessed May 12, 2017).
[67] B. Maggio, T. Ariga, R.K. Yu, Ganglioside GD3 lactones: polar head group mediated control of the intermolecular organization, Biochemistry 29 (1990) 8729–8734 http://www.ncbi.nlm.nih.gov/pubmed/2271553.
[68] B. Maggio, T. Ariga, R.O. Calderón, R.K. Yu, Ganglioside GD3 and GD3-lactone mediated regulation of the intermolecular organization in mixed monolayers with dipalmitoylphosphatidylcholine, Chem. Phys. Lipids 90 (1997) 1–10, http://dx.doi.org/10.1016/S0009-3084(97)00090-X.
[69] D.S. Patel, S. Park, E.L. Wu, M.S. Yeom, G. Widmalm, J.B. Klauda, W. Im, Influence of ganglioside GM1 concentration on lipid clustering and membrane properties and curvature, Biophys. J. 111 (2016) 1987–1999, http://dx.doi.org/10.1016/j.bpj.2016.09.021.
[70] O.G. Mouritsen, L.A. Bagatolli, Soft shells shape up, Life as a Matter Fat, Springer International Publishing, 2016, pp. 65–73, , http://dx.doi.org/10.1007/3-540-27076-0_7.
[71] B. Maggio, Geometric and thermodynamic restrictions for the self-assembly of glycosphingolipid-phospholipid systems, Biochim. Biophys. Acta 815 (1985) 245–258 http://www.ncbi.nlm.nih.gov/pubmed/3995027.
[72] M.A. Perillo, N.J. Scarsdale, R.K. Yu, B. Maggio, Modulation by gangliosides of the lamellar-inverted micelle (hexagonal II) phase transition in mixtures containing phosphatidylethanolamine and dioleoylglycerol, Proc. Natl. Acad. Sci. U. S. A. 91 (1994) 10019–10023, http://dx.doi.org/10.1073/pnas.91.21.10019.
[73] B. Maggio, F.A. Cumar, R. Caputto, Induction of membrane fusion by polysialogangliosides, FEBS Lett. 90 (1978) 149–152 http://www.ncbi.nlm.nih.gov/pubmed/658432.
[74] F.A. Cumar, B. Maggio, R. Caputto, Dopamine release from nerve endings induced by polysialogangliosides, Biochem. Biophys. Res. Commun. 84 (1978) 65–69 http://www.ncbi.nlm.nih.gov/pubmed/728135.
[75] C.G. Monferrán, B. Maggio, G.A. Roth, F.A. Cumar, R. Caputto, Membrane instability induced by purified myelin components. Its possible relevance to experimental allergic encephalomyelitis, Biochim. Biophys. Acta Biomembr. 553 (1979) 417–423, http://dx.doi.org/10.1016/0005-2736(79)90297-9.
[76] B. Maggio, Control by ganglioside GD1a of phospholipase A 2 activity through modulation of the lamellar-hexagonal (HII) phase transition, Mol. Membr. Biol. 13 (1996) 109–112, http://dx.doi.org/10.3109/09687689609160584.
[77] A. Sáez-Cirión, G. Basáñez, G. Fidelio, F.M. Goñi, B. Maggio, A. Alonso, Sphingolipids (galactosylceramide and sulfatide) in lamellar-hexagonal phospholipid phase transitions and in membrane fusion, Langmuir 16 (2000) 8958–8963, http://dx.doi.org/10.1021/la000532t.
[78] L.A. Bagatolli, E. Gratton, Two-photon fluorescence microscopy observation of shape changes at the phase transition in phospholipid giant unilamellar vesicles, Biophys. J. 77 (1999) 2090–2101, http://dx.doi.org/10.1016/S0006-3495(99)77050-5.
[79] J. Juhasz, J.H. Davis, F.J. Sharom, Fluorescent probe partitioning in giant unilamellar vesicles of “lipid raft” mixtures, Biochem. J. 430 (2010) 415–423, http://dx.doi.org/10.1042/BJ20100516.